

Christopher Bräsen · Peter Schönheit

AMP-forming acetyl-CoA synthetase from the extremely halophilic archaeon *Haloarcula marismortui*: purification, identification and expression of the encoding gene, and phylogenetic affiliation

Received: 3 November 2004 / Accepted: 30 March 2005 / Published online: 10 June 2005
© Springer-Verlag 2005

Abstract Halophilic archaea activate acetate via an (acetate)-inducible AMP-forming acetyl-CoA synthetase (ACS), (Acetate + ATP + CoA \rightarrow Acetyl-CoA + AMP + PP_i). The enzyme from *Haloarcula marismortui* was purified to homogeneity. It constitutes a 72-kDa monomer and exhibited a temperature optimum of 41°C and a pH optimum of 7.5. For optimal activity, concentrations between 1 M and 1.5 M KCl were required, whereas NaCl had no effect. The enzyme was specific for acetate (100%) additionally accepting only propionate (30%) as substrate. The kinetic constants were determined in both directions of the reaction at 37°C. Using the N-terminal amino acid sequence an open reading frame — coding for a 74 kDa protein — was identified in the partially sequenced genome of *H. marismortui*. The function of the ORF as *acs* gene was proven by functional overexpression in *Escherichia coli*. The recombinant enzyme was reactivated from inclusion bodies, following solubilization in urea and refolding in the presence of salts, reduced and oxidized glutathione and substrates. Refolding was dependent on salt concentrations of at least 2 M KCl. The recombinant enzyme showed almost identical molecular and catalytic properties as the native enzyme. Sequence comparison of the *Haloarcula* ACS indicate high similarity to characterized ACSs from bacteria and eukarya and the archaeon *Methanosaeta*. Phylogenetic analysis of ACS sequences from all three domains revealed a distinct archaeal cluster suggesting monophyletic origin of archaeal ACS.

Keywords Acetate activation · AMP-forming acetyl-CoA synthetase · Halophilic archaea · *Haloarcula marismortui* · ACS evolution

Introduction

Acetate serves as substrate for catabolism and anabolism in several aerobic and anaerobic microorganisms. Prior to its utilization in metabolism, acetate has to be activated to acetyl-CoA, an important intermediate in various metabolic pathways, e.g. the citric acid cycle. The most common enzyme catalyzing the activation of acetate to acetyl-CoA is the AMP-forming acetyl-CoA synthetase (ACS) (acetate + ATP + CoA \rightarrow acetyl-CoA + AMP + PP_i). This mechanism of acetate activation is ubiquitous in all three domains of life and was described particularly for eukaryotes and for aerobic and facultative bacteria, e.g. *Escherichia coli*, as well as for the anaerobic archaeon *Methanosaeta* (Kumari et al. 1995; Thauer 1988; Jetten et al. 1992). Only few bacteria devoid of ACS, e.g. *Corynebacterium glutamicum*, and also the euryarchaeal *Methanosarcina* species activate acetate to acetyl-CoA via acetate kinase (AK) and phosphotransacetylase (PTA) or — as reported for few sulfate reducers — via a succinyl-CoA: acetate CoA transferase (Thauer et al. 1989; Gerstmeir et al. 2003; Aceti and Ferry 1988).

In archaea, except for the anaerobic acetoclastic methanogens, little information about acetate metabolism was available. Previously, halophilic archaea and the thermoacidophile *Sulfolobus acidocaldarius* were described to grow on acetate as carbon and energy source and the operation of glyoxylate cycle as anaplerotic sequence in these aerobic organisms was demonstrated (Serrano and Bonete 2001; Serrano et al. 1998; Uhrigshardt et al. 2002). However, the mechanism of acetate activation in aerobic archaea has not been analyzed. Recently, we performed detailed growth studies with various halophilic archaea, in particular with *Haloarcula*

Communicated by G. Antranikian

C. Bräsen · P. Schönheit (✉)
Institut für Allgemeine Mikrobiologie,
Christian-Albrechts-Universität Kiel,
Am Botanischen Garten 1-9, 24118 Kiel, Germany
E-mail: peter.schoenheit@ifam.uni-kiel.de
Tel.: +49-431-8804328
Fax: +49-431-8802194

marismortui, on acetate as carbon and energy source and presented evidence that acetate activation in these organisms is catalyzed by an acetate-inducible ACS.

Acetate-grown *Haloarcula* cells also contained an ADP-forming acetyl-CoA synthetase (ACD), which — in contrast to ACS — catalyzes the ADP-dependent interconversion of acetyl-CoA to acetate (acetyl-CoA + ADP + $p_i \rightleftharpoons$ acetate + ATP + CoA). Although this enzyme catalyzes a reversible reaction in vitro, our data clearly indicate that in vivo ACD operates exclusively in the direction of acetate formation (Bräsen and Schönheit 2001; Bräsen and Schönheit 2004; FEMS Microbiol. Lett., in press). It was discussed that this functional difference might be due to the higher acetate affinity of ACS compared to ACD.

So far, ACS has been characterized mainly from bacteria and eukarya and, recently, the first crystal structures of ACS, from the bacterium *Salmonella enterica* and from *Saccharomyces cerevisiae* were reported (Gulick et al. 2003; Jogl and Tong 2004). The enzyme catalyzes the ATP- and CoA-dependent activation of acetate to acetyl-CoA, yielding AMP and PP_i in a two step reaction with acetyl-AMP as intermediate (Gulick et al. 2003):

1. Acetate + ATP \rightarrow acetyl-AMP + PP_i
2. Acetyl-AMP + CoA \rightarrow acetyl-CoA + AMP.

The enzyme has recently generated considerable interest due to its medical importance in mammals, where it is involved in fatty acid and cholesterol biosynthesis (Ikeda et al. 2001; Luong et al. 2000). Furthermore, posttranslational regulation of ACS by acetylation/deacetylation of a highly conserved lysine residue involving sirtuins, has recently been reported (Starai et al. 2002, 2003; Smith et al. 2000). So far, this kind of regulation has been described in detail for histone proteins and transcription-related factors (Sterner and Berger 2000).

Thus, while there is growing information about ACSs in eukarya and bacteria, little information about archaeal ACSs and their encoding genes was available and also the phylogenetic affiliation remained unclear. In this paper, we report the molecular and biochemical characterization of ACS from the aerobic euryarchaeon *H. marismortui* and the identification of its encoding gene (*acs*) in the partially sequenced genome of this organism. Furthermore, a sequence comparison of the *Haloarcula* ACS with other characterized ACS was performed and its phylogenetic affiliation was analyzed including various archaeal ACS homologs available from genome sequences. The data suggest a monophyletic origin of archaeal ACS.

Materials and methods

Purification of ACS from *H. marismortui* and N-terminal amino acid sequencing

Haloarcula marismortui DSM 5350 (Oren et al. 1990) was grown in a 50-l Biostat fermentor with an acetate-

containing medium (for detailed description of the media see Bräsen and Schönheit, 2001). Cell extracts were prepared from 30 g (wet weight) of frozen acetate grown cells, which were suspended in buffer containing 50 mM Tris-HCl pH 7.0 and 200 g l⁻¹ NaCl. Cells were disrupted by passing through a French pressure cell at 1.3×10^8 Pa. Cell debris was removed by centrifugation for 90 min at 100,000 g. The supernatant was incubated at 70°C for 20 min followed by an additional centrifugation step at 100,000 g for 90 min. The supernatant was dialysed with 50 mM Tris-HCl pH 7.0 containing 20 mM MgCl₂ 10% (v/v) glycerol (buffer A). The protein solution was applied to a Q-Sepharose HiLoad 26/10 equilibrated with buffer A. Protein was desorbed at a flow rate of 1 ml min⁻¹ with buffer A containing 0.3 M NaCl followed by a linear gradient from 0.3 M to 0.5 M NaCl. The fractions with the highest ACS activity (0.36–0.41 M NaCl) were pooled, adjusted to a final concentration of 2 M (NH₄)₂SO₄ and applied to a Phenyl-Sepharose HiLoad 16/10 equilibrated with buffer A, containing 2 M (NH₄)₂SO₄. Protein was eluted with buffer A containing 1.76 M (NH₄)₂SO₄ at a flow rate of 1 ml min⁻¹ followed by a linear gradient from 1.76 to 0.8 M (NH₄)₂SO₄. The fractions containing the highest ACS activity (1.6–1.2 M (NH₄)₂SO₄) were pooled, concentrated by ultrafiltration with Amicon ultrafiltration cell 8010 (cutoff of 30 kDa) and applied to a Superdex 200 HiLoad 16/60 equilibrated with buffer A containing 2 M NaCl. The protein was eluted at a flow rate of 1 ml min⁻¹. The fractions containing the highest ACS activity were eluted between 76 ml and 81 ml. At this stage ACS was essentially pure.

N-terminal amino acid sequencing was carried out by analyzing the purified ACS on a 13% polyacrylamide gel in the presence of 6 M urea (Schaeffer and von Jagow 1987). Blotting onto a polyvinylidene difluoride membrane and N-terminal microsequencing on a model 473A sequencer (Applied Biosystems) were performed as described by Meyer et al. (1996).

Cloning and expression of *H. marismortui* ACS in *E. coli*

In contig 147 of the partially sequenced genome of *H. marismortui* (Zhang et al. 2003) the gene putatively encoding the ACS was identified by BLAST search using the N-terminal amino acid sequence of the purified enzyme. The ORF, designated *acs*, was amplified from genomic DNA of *H. marismortui* by PCR. The PCR product was cloned into pET17b (Novagene) via two restriction sites (*Nde*I and *Xho*I) created with the primers 5'-CGATGATAGCATATGTCAGATGAAGAT-GTC C-3' and 5'-CGTGGTGCTG CTCTGAG-GTTAGGG-3'. For expression, *E. coli* BL21 codon plus(DE3)-RIL cells (Stratagene) transformed with vector pET17b-*acs*Har were grown in Luria-Bertani medium at 37°C. The expression was started by inducing the promoter with 0.4 mM isopropyl-1-thio-β-D-galactopyranoside

(IPTG). After 3 h of further growth, cells were harvested by centrifugation.

Solubilization, refolding and purification of recombinant *H. marismortui* ACS

Refolding of the insoluble recombinant ACS was performed using a modified method according to Connaris et al. (1999). *E. coli* BL21 codon plus(DE3)-RIL cell pellets, transformed with pET17b-*acsHar*, were resuspended in 20 mM Tris-HCl buffer, pH 7.5, containing 2 M KCl and 2 mM EDTA (buffer B), treated with 100 $\mu\text{g ml}^{-1}$ lysozyme and 0.1 volume of 1% (v/v) Triton-X100 and incubated at 30°C for 1 h before transferring the solution onto ice for 15 min. The suspension was then sonicated and centrifuged at 40,000 $\times g$ for 30 min at 4°C. The pellet was washed twice in buffer B and centrifuged as before. The insoluble fraction was dissolved in solubilization buffer (20 mM Tris-HCl, pH 7.5, containing 8 M urea, 2 mM EDTA, 50 mM DTE). Refolding was initiated by slowly diluting the solubilized pellet into reactivation buffer to a final protein concentration of 0.03 mg ml^{-1} followed by incubation for 60 h at 4°C. The reactivation buffer was composed of buffer B supplemented with 2 mM ATP, 2.5 mM sodium acetate, 10 μM CoA, 3 mM reduced glutathione (GSH) and 0.3 mM oxidized glutathione (GSSG).

The renatured protein was concentrated by ultrafiltration (cutoff 30 kDa) and adjusted to 2 M $(\text{NH}_4)_2\text{SO}_4$. The protein solution was then centrifuged at 100,000 g for 45 min at 4°C. The supernatant was applied to a Phenyl-Sepharose 6ff (low sub) (1 ml) equilibrated with 50 mM Tris-HCl, pH 7.5 (buffer C), containing 20 mM MgCl_2 and 2 M $(\text{NH}_4)_2\text{SO}_4$. Protein was desorbed with buffer C containing 20% glycerol (v/v) at a flow rate of 1 ml min^{-1} with a decreasing gradient from 2 M $(\text{NH}_4)_2\text{SO}_4$ to 0 M $(\text{NH}_4)_2\text{SO}_4$. The fractions with the highest ACS activity were concentrated by ultrafiltration and applied to a Superdex 200 HiLoad 16/60 equilibrated with buffer C, containing 2 M KCl, 20 mM MgCl_2 and 10% glycerol (v/v). Protein was eluted at a flow rate of 1 ml min^{-1} and the eluted ACS was essentially pure.

Characterization of ACS from *H. marismortui*

Enzyme assays

Acetyl-CoA synthetase (AMP-forming) (acetate + HSCoA + ATP \rightarrow acetyl-CoA + AMP + PP_i) was measured under aerobic conditions at 37°C using three different assay systems (A, B, C): (A) The formation of acetyl-CoA from acetate, ATP and HSCoA was assayed according to Aceti and Ferry (1988) by monitoring the acetyl-hydroxamate formation from acetyl-CoA and hydroxylamine at 540 nm. The assay mixture contained 100 mM Tris-HCl pH 7.5, 30 mM MgCl_2 , 400 mM potassium acetate, 700 mM hydroxylamine hydrochloride, 10 mM ATP and

1 mM HSCoA. This assay was used to measure the ACS activity during the purification procedure. (B) The HSCoA and acetate dependent AMP formation from ATP was measured by coupling the reaction with the oxidation of NADH at 365 nm via pyruvate kinase, lactate dehydrogenase and adenylate kinase according to Oberlies et al. (1980). The assay mixture contained 100 mM Tris-HCl pH 7.5, 1.25 M KCl, 5 mM MgCl_2 , 2.5 mM sodium acetate, 2 mM ATP, 1 mM HSCoA, 2.5 mM phosphoenolpyruvate, 0.3 mM NADH, 6 U lactate dehydrogenase, 4 U pyruvate kinase and 13.6 U adenylate kinase. This assay was used (1) to determine the apparent K_m values for acetate, ATP and HSCoA, (2) to test the specificity of the enzyme for organic acids and phosphoryl donors and (3) to determine the salt dependence and the salt stability. The auxiliary enzymes were tested to ensure that they were not rate limiting. (C) The PP_i and AMP dependent HSCoA release from acetyl-CoA was monitored according to Srere et al. (1963) with Ellman's thiol reagent, 5'-dithiobis (2-nitrobenzoic acid) (DTNB), by measuring the formation of thiophenolate anion at 412 nm ($\epsilon_{412} = 13.6 \text{ mM}^{-1} \text{ cm}^{-1}$). The assay mixture contained 20 mM Tris-HCl pH 7.5, 1.25 M KCl, 2.5 mM MgCl_2 , 0.1 mM DTNB, 1.5 mM acetyl-CoA, 2 mM AMP and 2 mM PP_i . This assay was used to determine (1) the K_m values for acetyl-CoA, AMP and PP_i , (2) the substrate specificities for nucleoside monophosphates and (3) the pH and temperature optima of ACS.

pH and temperature dependence, salt effects and substrate specificity

The pH dependence of ACS was determined between pH 5.0 and pH 9.0 in the direction of acetate formation with Ellman's thiol reagent according to Srere et al. (1963) using either morpholine-ethane sulfonic acid (MES) (pH 5.0–7.0) or Tris-HCl (pH 7.0–9.0) (each 20 mM).

The temperature dependence of the enzymes were determined between 17°C and 45°C in the direction of acetate formation using the same assay systems as for the pH dependence.

The salt dependence of the enzyme activity was measured between 0 and 3 M KCl and NaCl, respectively, and between 0 mM and 150 mM MgCl_2 in the assay systems described above.

The substrate specificities ACS was examined in the direction acetyl-CoA formation replacing acetate with 2.5 mM formate, propionate, butyrate, fumarate, succinate, isobutyrate, isovalerate, phenylacetate, indol-3-acetate or benzoate.

Analytical assays

The purity of the preparations was documented by sodium dodecyl sulfate-polyacrylamide gel electrophoresis (SDS-PAGE) on a 12% polyacrylamide gel stained with Coomassie brilliant blue R250 (Laemmli 1970). Protein

concentrations were determined by the method of Bradford with bovine serum albumin as standard (Bradford 1976). Gel filtration chromatography was carried out as described above using HMW and LMW calibration kits (Amersham Bioscience, Amersham, England) as standard.

Sequence handling

Sequence alignments were constructed with the neighbor-joining method of ClustalX (Thompson et al. 1997) using the gonnet matrix options. Phylogenetic trees were constructed using both the neighbor-joining methods of ClustalX and the maximum likelihood phylogenetic analysis of TREE-PUZZLE 5.1 carried out by quartet-puzzling (Schmidt et al. 2002).

Results

Purification of ACS

The ACS was purified 268-fold from cell extracts of acetate-grown *H. marismortui* by anion exchange chromatography on Q-Sepharose, hydrophobic interaction chromatography on Phenyl-Sepharose and gel filtration chromatography on Superdex 200 to a specific activity of 13 U mg⁻¹ (at 37°C) with a yield of 28% (Table 1). The purified protein was apparently homogenous as judged by

denaturing SDS-PAGE (Fig. 1). ACS thus represents about 0.4% of the cellular protein of *H. marismortui*.

Molecular and catalytic properties

The apparent molecular mass of native ACS, determined by gel filtration on Superdex 200, was approximately 72 kDa. SDS-PAGE revealed only one subunit with an apparent molecular mass of 89 kDa (Fig. 1), suggesting a monomeric (α) structure of the native enzyme.

Kinetic parameters of native and recombinant ACS were determined at 37°C (Table 2). In both directions of the reaction the rate dependence followed Michaelis-Menten kinetics. The apparent V_{\max} and K_m values in the direction of acetyl-CoA formation were 26.5 U mg⁻¹, 0.23 mM (acetate), 0.38 mM (HSCoA) and 0.56 mM (ATP) respectively, and in the direction of acetate formation 6.2 U mg⁻¹, 0.41 mM (acetyl-CoA), 0.25 mM (AMP) and 0.38 mM (PP_i) respectively. The pH optimum of ACS was at pH 7.5 with about 30%–40% remaining activity at pH 6.5 and 8.5. The temperature optimum was at 41°C (Fig. 2). From the linear part of the Arrhenius plot between 24°C and 37°C an activation energy of 90 kJ mol⁻¹ was calculated.

Effect of salts

The effect of KCl and NaCl on the enzyme activity was tested between 0 M and 3 M in the presence of 5 mM

Table 1 Purification of ACS from *H. marismortui*. Enzyme activity was measured at 37°C in the direction of acetyl-CoA formation using the hydroxamate assay as described in materials and methods. 1 U = 1 μ mol acetyl hydroxamate formed per minute

Purification step	Protein (mg)	Activity (U)	Specific activity (U/mg)	Yield (%)	Purification (-fold)
Cell-free extract	1,705	85	0.05	100	1.0
Heat precipitation	755	186	0.25	216	4.9
Q sepharose	39.8	106	2.66	125	53.2
Superdex 200	4.93	42	8.5	49	169.0
Phenyl sepharose	1.79	24	13.4	28	268.0

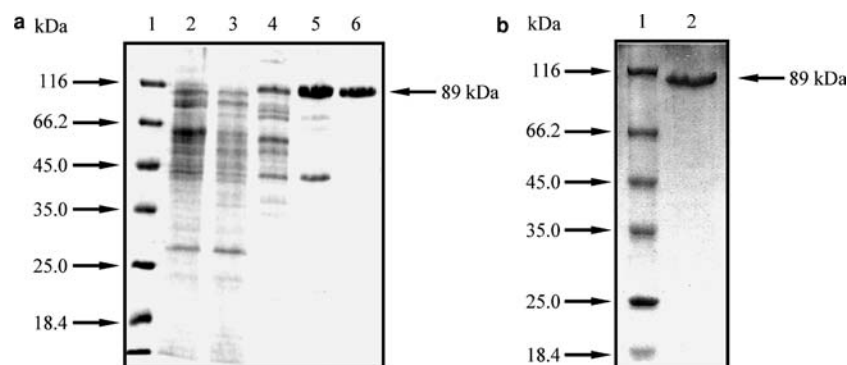


Fig. 1 Purification of AMP-forming acetyl-CoA synthetase (ACS) from *Haloarcula marismortui* (a) and of recombinant ACS from transformed *Escherichia coli* (b) as analyzed by SDS-PAGE. a Lane 1, molecular mass standards (Sigma) kDa; lane 2, cell-free extract;

lane 3, heat precipitation; lane 4 Q Sepharose; lane 5, Superdex 200; lane 6, Phenyl Sepharose. b Lane 1, molecular mass standard; lane 2, purified recombinant ACS

Table 2 Molecular and catalytic properties of native and recombinant ACS from *H. marismortui*. Kinetic constants were determined both in the direction of acetyl-CoA formation and acetate formation as described in materials and methods. The molecular mass of native enzyme was determined by gel filtration, of subunit by SDS-PAGE

	Substrate	Native enzyme	Recombinant enzyme
Apparent molecular mass of enzyme (kDa)			
Native		72	72
Subunit		89	89
Calculated		—	74
Oligomeric structure		α	α
Apparent V_{\max} value (U/mg) (direction of acetyl-CoA formation)		26	26
Apparent K_m value (mM)	Acetate	0.23	0.36
	ATP	0.56	0.35
	CoA-SH	0.38	0.31
Apparent V_{\max} value (U/mg) (direction of acetate formation)		6.2	4.1
Apparent K_m value (mM)	Acetyl-CoA	0.41	1.08
	AMP	0.25	0.36
	PP _i	0.38	0.43
pH optimum		7.5	ND
Temperature optimum (°C)		41	ND
Arrhenius activation energy (25–39°C) (kJ/mol)		97	ND

ND not determined

MgCl₂ (Fig. 3). The enzyme showed highest activity between 1.0 M and 1.5 M KCl (optimum at 1.25 M) and 50% and 60% remaining activity was observed at KCl concentrations of 0.5 M and 2.5 M, respectively. When KCl was replaced by NaCl in concentrations from 0.5 M to 3 M only 20% of the maximal activity was found. The optimal MgCl₂ concentration for ACS activity was determined in the presence of 1.25 M KCl. Optimal activity was reached between 3.5 mM and 15 mM MgCl₂ (optimum at 5 mM). In the absence of KCl only 4% remaining activity was observed with 5 mM MgCl₂.

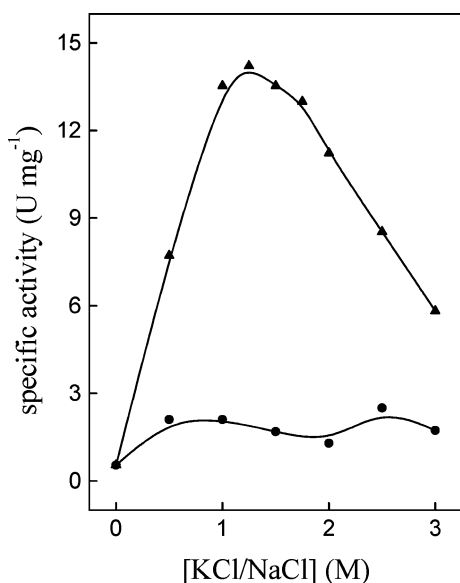


Fig. 2 Effect of KCl (filled triangle) and NaCl (filled circle) concentrations on the specific activity of purified AMP-forming acetyl-CoA synthetase (ACS) from *H. marismortui*

Substrate specificities

Various organic acids were tested as substrates for ACS. In addition to acetate (100%) only propionate (32%) was accepted with significantly reduced activity. In the opposite direction the enzyme showed highest activity with acetyl-CoA and AMP (100%). AMP could not be substituted with GMP. ADP could not serve as phosphoryl acceptor clearly defining the enzyme as AMP-forming.

Identification, functional overexpression of the gene encoding ACS in *H. marismortui*

Using the N-terminal amino acid sequence determined for the purified enzyme (MDEDVQLEARLEE-QEVFE), an open reading frame, which exactly matches the 18 amino acids was identified in contig 147 of partially sequenced genome of *H. marismortui*. The ORF consists of 1995 bp coding for a polypeptide of 664 amino acids with a calculated molecular mass of 74.2 kDa. The protein contains high amounts of negatively charged amino acids, 11% Asp and 11% Glu, which is typical for halophilic enzymes and had a predicted pI of 3.9. The G + C content of the *acs* gene is 62 mol%. The coding sequence starts with ATG and stops with TGA. The ORF was identified as *acs* gene encoding ACS by its functional overexpression in *E. coli*. The *acs* gene was amplified by PCR, cloned into vector pET17b and the recombinant plasmid was used to transform *E. coli* BL21 codon plus (DE3)-RIL. After induction with IPTG a polypeptide of about 89 kDa was overproduced, almost completely in form of inclusion bodies. The protein was purified from inclusion bodies as catalytic-active, extremely halophilic ACS as follows.

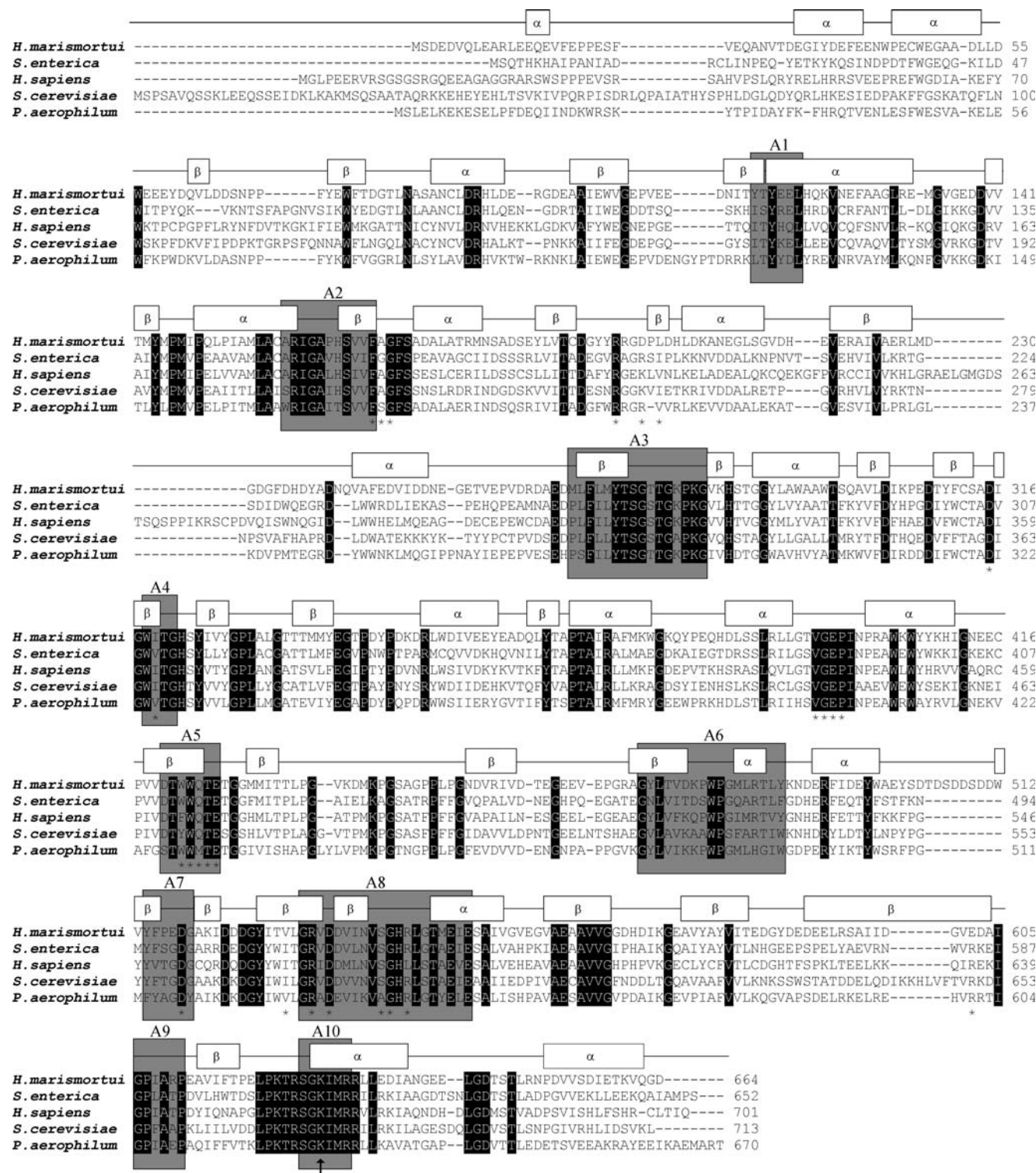


Fig. 3 Multiple sequence alignment of amino acid sequences of AMP-forming acetyl-CoA synthetase (ACS) from eukarya, bacteria and archaea. The alignment was generated with ClustalX using the gonnet matrix. The predicted secondary structure of the ACS from *H. marismortui* is shown above the sequences. Residues proposed to take part in substrate binding as deduced from the *Salmonella enterica* X-ray structure are indicated by asterisks. The

arrow indicates the lysine residue essential for catalysis and posttranslational regulation. The ten conserved regions described for the acyl-adenylate/thioester forming enzyme family are highlighted by shaded boxes. NCBI accession numbers: *Homo sapiens*, NP_061147; *Pyrobaculum aerophilum* strain IM2, NP_560315; *Salmonella enterica* serovar typhimurium LT2, Q8ZKF6; *Saccharomyces cerevisiae*, S30019

Reactivation, purification and characterization of recombinant ACS

Recombinant ACS was purified from inclusion bodies by dissolving in 8 M urea in the presence of DTE, followed by refolding in buffer containing high salt concentration (2 M KCl), substrates and glutathione (see Materials and Methods). Maximal ACS activity was achieved after 60 h of incubation at 4°C. The reactivated recombinant ACS was purified by ammonium sulfate precipitation, hydrophobic interaction chromatography on phenyl sepharose and gel filtration. The recombinant ACS purified from transformed *E. coli* and native ACS purified from *H. marismortui* showed almost identical properties, including molecular masses of enzyme and subunits, apparent V_{\max} and K_m values and substrate specificities (Table 2).

Sequence comparison and phylogenetic affiliation

The amino acid sequence of the archaeal ACS from *H. marismortui* was compared with other characterized and putative ACSs from the domains of bacteria and eukarya. The haloarchaeal sequence showed a high degree of identity (>26%) to the other sequences and shared certain conserved sequence motifs (A1–A10) of the acyl-adenylate/thioester forming enzyme superfamily (Starai and Escalante-Semerena 2004a; Gulick et al. 2003). Furthermore, most of the residues shown to be involved in substrate binding, as concluded from the crystal structure of the *S. enterica* enzyme, and especially the lysine residue (K609) reported to be crucial for catalysis and to be the site for posttranslational acetylation/deacetylation are well conserved in the *H. marismortui* ACS (Gulick et al. 2003).

The *H. marismortui* ACS and various archaeal homologs, recently available from genome sequences, allowed a comprehensive analysis of ACS phylogeny including selected ACS sequences from bacteria and eukarya. The studies revealed that the selected ACS sequences clustered in two main groups, i.e. an eukaryotic and a prokaryotic group (Fig. 4). This overall topology of the phylogenetic tree was achieved by both neighbor-joining and maximum likelihood method and is supported by fairly good bootstrapping values. The eukaryotic group is further divided into two distinct clusters, one of which (Eukarya I) comprises the fungal sequences and the other (Eukarya II) those of animals and plants and, additionally, also the α - and γ -proteobacterial ACSs. Within the second, prokaryotic main group four distinct clusters could be distinguished: a β - and ϵ -proteobacterial and a cyanobacterial subgroup, a third cluster containing sequences from high G + C gram positive bacteria and a fourth cluster comprising all archaeal sequences. Thus, the archaeal sequences form a separate branch, which is more closely related to bacterial than to eukaryotic ACSs, suggesting a monophyletic origin of archaeal ACS.

Discussion

AMP-forming acetyl-CoA synthetase (ACS) represents the most important and common mechanism of acetate activation particularly in aerobic bacteria and eukarya. However, no characterization of ACS neither from an aerobic nor from an extremophilic archaeon has been reported.

In this communication, we present the first characterization of an extremophilic ACS, from the aerobic archaeon *H. marismortui*. Using the N-terminal amino acid sequences of the purified enzyme, the encoding gene was identified in the partially sequenced genome by functional overexpression in *E. coli*. The recombinant halophilic ACS, which had to be reactivated from inclusion bodies, showed almost identical molecular and kinetic properties as the native enzyme.

Furthermore, due to the sequence data recently available from archaeal genomes, the first comprehensive study on the phylogenetic affiliation of archaeal ACSs is reported, indicating a monophyletic origin of these enzymes in archaea.

Molecular and catalytic properties

Usually, ACSs are monomers or homodimers composed of about 70–75 kDa subunits and thus, the monomeric structure and the molecular mass of the haloarchaeal ACS corresponds to the monomeric enzymes characterized from *S. enterica*, *E. coli*, *Azotobacter aceti*, spinach, cow and human (Gulick et al. 2003; Kumari et al. 1995; O'Sullivan and Ettlinger 1976; Zeiher and Randall 1991; Ishikawa et al. 1995; Luong et al. 2000). The calculated molecular mass of 74.2 kDa of the halophilic enzyme corresponded well with the results obtained by gel filtration (72 kDa). However, using SDS-PAGE the apparent molecular mass was overestimated (89 kDa), a feature recently reported for several halophilic proteins including the ADP-forming acetyl-CoA synthetase and xylose dehydrogenase purified from *H. marismortui* (Bräsen and Schönheit 2004; Johnsen and Schönheit 2004). The overestimation has been attributed to the presence of high amounts of negatively charged amino acids typical for halophilic proteins (Bonete et al. 1996).

The *H. marismortui* ACS requires high salt concentration (optimal at 1.3 M KCl) for enzyme activity, which is in the same range as reported for other halophilic proteins, e.g. xylose dehydrogenase from *H. marismortui*, glucose and glutamate dehydrogenase from *Haloferax mediterranei* (Johnsen and Schönheit 2004; Bonete et al. 1996; Ferrer et al. 1996). In contrast to the latter proteins, NaCl could not substitute for KCl to activate ACS activity. ACS from *H. marismortui* also required high KCl concentrations (at least 2 M KCl) for reactivation after heterologous expression in *E. coli*. This is in good agreement with the view that halophilic



Fig. 4 Phylogenetic relationship of AMP-forming acetyl-CoA synthetases (ACS) from eukarya, bacteria and archaea. The numbers at the nodes are bootstrapping values according to neighbor-joining [generated by using the neighbor-joining algorithm of ClustalX (Thompson et al. 1997)]. NCBI accession numbers: *A. pernix*, *Aeropyrum pernix* K1 NP_147884; *A. fulgidus*, *Archaeoglobus fulgidus* NP_069202; *A. thal.*, *Arabidopsis thaliana* NP_198504; *A. var.*, *Anabaena variabilis* ATCC29413 ZP_00158782; *B. pert.*, *Bordatella pertussis* NP_881040; *B. taurus* (Mito.), *Bos taurus* (mitochondrial ACS) NP_777171; *B. japonicum*, *Bradyrhizobium japonicum* USDA 110 AAK95494; *C. elegans*, *Caenorhabditis elegans* NP_497782; *C. jej.*, *Campylobacter jejuni* subsp. *jejuni* str. NCTC 11168 NP_282668; *C. albic.*, *Candida albicans* CAA22000; *C. parvum*, *Cryptosporidium parvum* Q27549; *D. melano.*, *Drosophila melanogaster* S52154; *E. nid.*, *Emeritica nidulans* CAA34858; *E. coli*, *Escherichia coli* K12 AAC77039; *F. acid.*, *Ferropasma acidarmanus* ZP_00000146; *G. violac.*, *Gloeobacter violaceus* PCC7421 NP_923105; *H. maris.*, *Haloarcula marismortui* (<http://zdna2.umbi.umd.edu/>); *Hf. vol.*; *Haloferax volcanii* (<http://zdna2.umbi.umd.edu/>); *NRC-1*, *Halobacterium* sp. NRC-1 NP_279934; *H. pyl.*, *Helicobacter pylori* 26695 NP_207835; *H. sapiens*, *Homo sapiens* (cytoplasmatic ACS) NP_061147; *H. sapiens* (Mito.), *Homo sapiens* (mitochondrial ACS) Q9NUI1; *K. lactis*, *Kluyveromyces lactis* AAC16713; *K. ra.*, *Kineococcus radiotolerans* (http://genome.jgi-psf.org/draft_microbes/kinra/kinra).

ra.home.html); *M. avi.*, *Mycobacterium avium* subsp. *paratuberculosis* str. k10 NP_959341; *Mc. burt.*, *Methanococcoides burtonii* DSM6242 ZP_00148668; *M. concilii*, *Methanoseta concilii* AAA73007; *M. maripa*, *Methanococcus maripaludis* S2 NP_987268; *M. mus.*, *Mus musculus* (cytoplasmatic ACS) Q9QXG4; *M. mus.* (Mito.), *Mus musculus* (mitochondriale ACS) NP_542142; *M. tub.*, *Mycobacterium tuberculosis* H37Rv NP_218184; *N. cras.*, *Neurospora crassa* SYNCAA; *N. puncti.*, *Nostoc punctiforme* PCC73102 ZP_00108549; *P. chry.*, *Penicillium chrysogenum* JN0781; *P. aeroph.*, *Pyrobaculum aerophilum* strain IM2 NP_560315; *P. marin.*, *Prochlorococcus marinus* subsp. *pastoris* str. CCMP1986 NP_892737; *P. torridus*, *Picrophilus torridus* DSM9790 YP_023061; *W. eutro.*, *Wautersia eutropha* P31638; *R. norv.*, *Rattus norvegicus* XP_230773; *R. caps.*, *Rhodobacter capsulatus* T03473; *S. cerevisiae*, *Saccharomyces cerevisiae* (cytoplasmatic ACS) NP_013254; *S. ent.*, *Salmonella enterica* serovar *typhimurium* LT2 Q8ZKF6; *S. tubero.*, *Solanum tuberosum* CAA67130; *S. co.*, *Streptomyces coelicolor* A3(2) NP_627761; *S. solf.*, *Sulfolobus solfataricus* NP_344180; *S. toko.*, *Solfobolus tokodaii* NP_378009; *Synecho.*, *Synechocystis* sp. PCC6803 Q55404; *T. acido.*, *Thermoplasma acidophilum* NP_393899; *T. fu.*, *Thermobifida fusca* ZP_00293126; *T. volc.*, *Thermoplasma volcanium* BAB60317; *W. succ.*, *Wolinella succinogenes* DSM1740 NP_906827. The scale bar corresponds to 0.1 substitutions per site

proteins unfold below salt concentrations of 2 M KCl (Madern et al. 2000) and was also described for recombinant xylose dehydrogenase from *H. marismortui* as well as citrate synthase and dihydrolipoamide dehydrogenase from *Haloferax volcanii* (Johnsen and Schönheit 2004; Connaris et al. 1999). These halophilic properties including the significantly higher content in

negatively charged amino acid residues, also reported for most other halophilic proteins, reflect the high intracellular salt concentrations present in haloarchaea (Madern et al. 2000).

The *H. marismortui* ACS as most of the other characterized ACSs was shown to be specific for acetate. In addition to acetate (100%), only propionate (30%) is

accepted as substrate with significantly reduced efficiency suggesting a pivotal role of this enzyme in acetate activation rather than in metabolism of short chain fatty acids in general. Only the enzyme from *Penicillium chrysogenum* was described to have a broader substrate spectrum and a role of this enzyme in providing activated side chains in the synthesis of antibiotics was discussed (Martinez-Blanco et al. 1992).

The substrate affinities, particularly the apparent K_m value for acetate (0.23 mM) of ACS from *H. marismortui* are similar to those of other ACS. However, the value is about ten-fold lower than that for ADP-forming acetyl-CoA synthetase (ACD) (2.6 mM) from the same organism, which catalyzes the ADP-dependent formation of acetate (acetyl-CoA + ADP + $p \rightleftharpoons$ acetate + ATP + CoA) during exponential growth on glucose (Bräsen and Schönheit 2004). The higher affinity for acetate of the acetate activating ACS as compared to acetate forming ACD might explain the induction of ACS during growth of *H. marismortui* on acetate (Bräsen and Schönheit 2001). A similar situation has been found in bacteria, which activate acetate mainly by high-affinity ACS but form acetate by AK/PTA, which exhibit a comparably high K_m value for acetate as ACD in archaea. Furthermore, the high affinity of ACS for acetate in *H. marismortui* enable the organism to effectively activate acetate in natural, hypersaline environments, where acetate is present at low concentrations (Oren 1995).

Sequence comparison and phylogenetic affiliation

As shown in the sequence alignment in Fig. 3, ACS from *H. marismortui* shows a high degree of identity to other ACSs from the domains of bacteria and eukarya (>26%) and share certain conserved sequence motifs (A1–A10) of the acyl-adenylate/thioester forming enzyme superfamily. Four of these conserved sequence motifs (A3, A5, A8, A10) were functionally characterized previously (Starai and Escalante-Semerena 2004a; Gulick et al. 2003). The A3 and A10 regions were described to be involved in the first half reaction, while the regions A5 and A8 were shown to take part in substrate binding of the second half reaction. Most of the residues shown to be involved in substrate binding, as concluded from the crystal structure of the *S. enterica* enzyme, and especially the catalytically essential lysine residue (K609) are well-conserved in the *H. marismortui* ACS (Gulick et al. 2003). This lysine residue has also been shown to be the site for post-translational regulation via acetylation/deacetylation (Starai et al. 2002, 2003). The mechanism of ACS acetylation at the lysine residue (K609) has recently been studied in *S. enterica* and the acetyl-CoA dependent protein acetyltransferase (Pat) was identified (Starai and Escalante-Semerena 2004b). Acetylation completely inhibits the first ACS half reaction and, thus, the mechanism of deacetylation is a prerequisite of ACS activity in vivo. Deacetylation of

lysine residue 609 in *S. enterica* and *S. cerevisiae* was shown to be catalyzed by sirtuins, which possess a NAD^+ -dependent deacetylase activity (Starai et al. 2002, 2003). Sirtuins were previously known to act mainly on histone proteins and, accordingly, have an important function in chromosome stabilization, gene silencing and cell aging (Starai et al. 2002; Smith et al. 2000). Since in *H. marismortui* ACS the lysine residue (K609) is also highly conserved (Fig. 3) and one putative sirtuin homolog was found in the partial sequenced genome, it is likely that this mechanism of post-translational regulation via acetylation/deacetylation also acts on the haloarchaeal enzyme characterized in this work.

However, a Pat enzyme homologous to that from *S. enterica* could not be identified in *H. marismortui* or in any of the available archaeal genome sequences, except for that of *Archaeoglobus fulgidus*. These findings suggest a type of protein acetyltransferase in archaea, which is different from that reported for the bacterium *S. enterica*.

Interestingly, the *S. enterica* Pat protein belong to the NDP-forming acyl-CoA synthetase enzyme superfamily, which also comprises ADP-forming acetyl-CoA synthetases (ACD) from archaea (Starai and Escalante-Semerena 2004b; Sanchez et al. 2000). It should be noted, that — in contrast to the acetate-activating ACS — ACDs catalyze the ADP-dependent formation of acetate from acetyl-CoA in *H. marismortui* and other archaea (Bräsen and Schönheit 2004).

Our analysis on the phylogenetic affiliation revealed that the selected ACS sequences clustered in two main groups, i.e. an eukaryotic and a prokaryotic group (Fig. 4). This overall topology of the phylogenetic tree and the division of the eukaryotic main group in a fungal subgroup (Eukarya I) and a cluster comprising ACS sequences of animals and plants is in good agreement with a previous work published by Karan et al. (2001) (Fig. 4). The relation between the latter eukaryotic subgroup and the α - and γ -proteobacterial ACSs, also obtained by our analysis, was considered to reflect the eubacterial origin of ACS in eukaryotes (Karan et al. 2001). However, it is interesting to note, that the mitochondrial sequences of human, mouse and cow clustered within in the fungal subgroup. This unexpected phylogenetic affiliation of nucleus-encoded mitochondrial sequences might be due to the different physiological function and to different modes of transcriptional regulation. In accordance, it was recently reported that the cytosolic and the mitochondrial ACS isoenzymes from mouse share only weak identity and that they belong to different phylogenetic groups (Fujino et al. 2001; Yamamoto et al. 2004).

The comparatively large set of archaeal ACS sequences, included in this work, formed a distinct cluster within the prokaryotic main group, additionally comprising three bacterial subgroups (β - and ϵ -Proteobacterial, Cyanobacteria, high G + C gram positive bacteria). Though, the bootstrap support of the inner

nodes within the prokaryotic main group is quite low, the topology of this group can be confirmed by including more sequences of each subgroup (data not shown). Moreover, the deep branching halophilic sequences and the apparent relationship to the sequences from the high G + C gram positive bacteria seems to contribute to the ambiguous position of the inner nodes and might be explained by the adaptation of halophilic ACSs to a high salt environment.

However, the phylogenetic tree, reported here, clearly demonstrates that the archaeal sequences form a separate branch, which is more closely related to bacterial than to eukaryotic ACSs, and support a monophyletic origin of archaeal ACS evolution.

Acknowledgements We thank Dr. R. Schmid (Osnabrück, Germany) for N-terminal amino acid sequencing of *H. marismortui* ACS. We also thank Dr. S. DasSarma for getting access to the *H. marismortui* genome data at the UMBI web site <http://zdna2.umbi.umd.edu/cgi-bin/blast/blast.pl> and the web site URL <http://zdna2.umbi.umd.edu/>.

References

- Aceti DJ, Ferry JG (1988) Purification and characterization of acetate kinase from acetate-grown *Methanosarcina thermophila*. Evidence for regulation of synthesis. *J Biol Chem* 263:15444–15448
- Bonete MJ, Pire C, Llorca FI, Camacho ML (1996) Glucose dehydrogenase from the halophilic Archaeon *Haloferax mediterranei*: enzyme purification, characterisation and N-terminal sequence. *FEBS Lett* 383:227–229
- Bradford MM (1976) A rapid and sensitive method for the quantitation of microgram quantities of protein utilizing the principle of protein-dye binding. *Anal Biochem* 72:248–254
- Bräsen C, Schönheit P (2001) Mechanisms of acetate formation and acetate activation in halophilic archaea. *Arch Microbiol* 175:360–368 (Erratum, 180:504, 2003)
- Bräsen C, Schönheit P (2004) Unusual ADP-forming acetyl-coenzyme A synthetases from the mesophilic halophilic euryarchaeon *Haloarcula marismortui* and from the hyperthermophilic crenarchaeon *Pyrobaculum aerophilum*. *Arch Microbiol* 182:277–287
- Connaris H, Chaudhuri JB, Danson MJ, Hough DW (1999) Expression, reactivation, and purification of enzymes from *Haloferax volcanii* in *Escherichia coli*. *Biotechnol Bioeng* 64:38–45
- Ferrer J, Perez-Pomares F, Bonete MJ (1996) NADP-glutamate dehydrogenase from the halophilic archaeon *Haloferax mediterranei*: enzyme purification, N-terminal sequence and stability. *FEMS Microbiol Lett* 141:59–63
- Fujino T, Kondo J, Ishikawa M, Morikawa K, Yamamoto TT (2001) Acetyl-CoA synthetase 2, a mitochondrial matrix enzyme involved in the oxidation of acetate. *J Biol Chem* 276:11420–11426
- Gerstmeir R, Wendisch VF, Schnicke S, Ruan H, Farwick M, Reinscheid D, Eikmanns BJ (2003) Acetate metabolism and its regulation in *Corynebacterium glutamicum*. *J Biotechnol* 104:99–122
- Gulick AM, Starai VJ, Horswill AR, Homick KM, Escalante-Semerena JC (2003) The 1.75 Å crystal structure of acetyl-CoA synthetase bound to adenosine-5'-propylphosphate and coenzyme A. *Biochemistry* 42:2866–2873
- Ikeda Y, Yamamoto J, Okamura M, Fujino T, Takahashi S, Takeuchi K, Osborne TF, Yamamoto TT, Ito S, Sakai J (2001) Transcriptional regulation of the murine acetyl-CoA synthetase 1 gene through multiple clustered binding sites for sterol regulatory element-binding proteins and a single neighboring site for Sp1. *J Biol Chem* 276:34259–34269
- Ishikawa M, Fujino T, Sakashita H, Morikawa K, Yamamoto T (1995) Kinetic properties and structural characterization of highly purified acetyl-CoA synthetase from bovine heart and tissue distribution of the enzyme in rat tissues. *Tohoku J Exp Med* 175:55–67
- Jetten MSM, Stams AJM, Zehnder AJB (1992) Methanogenesis from acetate: a comparison in *Methanotrix soehngenii* and *Methanosarcina* spp. *FEMS Microbiol Rev* 88:181–198
- Jogl G, Tong L (2004) Crystal structure of yeast acetyl-coenzyme A synthetase in complex with AMP. *Biochemistry* 43:1425–1431
- Johnsen U, Schönheit P (2004) Novel xylose dehydrogenase in the halophilic archaeon *Haloarcula marismortui*. *J Bacteriol* 186:6198–6207
- Karan D, David JR, Capy P (2001) Molecular evolution of the AMP-forming acetyl-CoA synthetase. *Gene* 265:95–101
- Kumari S, Tishel R, Eisenbach M, Wolfe AJ (1995) Cloning, characterization, and functional expression of *acs*, the gene which encodes acetyl coenzyme A synthetase in *Escherichia coli*. *J Bacteriol* 177:2878–2886
- Laemmli UK (1970) Cleavage of structural proteins during the assembly of the head of bacteriophage T4. *Nature* 227:680–685
- Luong A, Hannah VC, Brown MS, Goldstein JL (2000) Molecular characterization of human acetyl-CoA synthetase, an enzyme regulated by sterol regulatory element-binding proteins. *J Biol Chem* 275:26458–26466
- Madern D, Ebel C, Zaccai G (2000) Halophilic adaptation of enzymes. *Extremophiles* 4:91–98
- Martinez-Blanco H, Reglero A, Fernandez-Valverde M, Ferrero MA, Moreno MA, Penalva MA, Luengo JM (1992) Isolation and characterization of the acetyl-CoA synthetase from *Penicillium chrysogenum*. Involvement of this enzyme in the biosynthesis of penicillins. *J Biol Chem* 267:5474–5481
- Meyer C, Schmid R, Scriba PC, Wehling M (1996) Purification and partial sequencing of high-affinity progesterone-binding site(s) from porcine liver membranes. *Eur J Biochem* 239:726–731
- Oberlies G, Fuchs G, Thauer RK (1980) Acetate thiokinase and the assimilation of acetate in *Methanobacterium thermoautotrophicum*. *Arch Microbiol* 128:248–252
- Oren A (1995) Uptake and turnover of acetate in hypersaline environments. *FEMS Microbiol Ecol* 18:75–85
- Oren A, Ginzburg M, Ginzburg BZ, Hochstein LI, Volcani BE (1990) *Haloarcula marismortui* (Volcani) sp. nov., nom. rev., an extremely halophilic bacterium from the Dead Sea. *Int J Syst Bacteriol* 40:209–210
- O'Sullivan J, Ettlinger L (1976) Characterization of the acetyl-CoA synthetase of *Acetobacter aceti*. *Biochim Biophys Acta* 450:410–417
- Sanchez LB, Galperin MY, Müller M (2000) Acetyl-CoA synthetase from the amitochondriate eukaryote *Giardia lamblia* belongs to the newly recognized superfamily of acyl-CoA synthetases (nucleoside diphosphate-forming). *J Biol Chem* 275:5794–5803
- Schaeffer H, von Jagow G (1987) Tricine-sodium-dodecylsulfate-polyacrylamide gel electrophoresis for the separations of proteins in the range from 1–100 kDa. *Anal Biochem* 166:368–379
- Schmidt HA, Strimmer K, Vingron M, von Haeseler A (2002) TREE-PUZZLE: maximum likelihood phylogenetic analysis using quartets and parallel computing. *Bioinformatics* 18:502–504
- Serrano JA, Bonete MJ (2001) Sequencing, phylogenetic and transcriptional analysis of the glyoxylate bypass operon (*ace*) in the halophilic archaeon *Haloferax volcanii*. *Biochim Biophys Acta* 1520:154–162
- Serrano JA, Camacho M, Bonete MJ (1998) Operation of glyoxylate cycle in halophilic archaea: presence of malate synthase and isocitrate lyase in *Haloferax volcanii*. *FEBS Lett* 434:13–16
- Smith JS et al (2000) A phylogenetically conserved NAD⁺-dependent protein deacetylase activity in the Sir2 protein family. *Proc Natl Acad Sci USA* 97:6658–6663

- Srere PA, Brazil H, Gonen L (1963) The citrate condensing enzyme of pigeon breast muscle and moth flight muscle. *Acta Chem Scand* 17:129–134
- Starai VJ, Escalante-Semerena JC (2004a) Acetyl-coenzyme A synthetase (AMP forming). *Cell Mol Life Sci* 61:2020–2030
- Starai VJ, Escalante-Semerena JC (2004b) Identification of the protein acetyltransferase (Pat) enzyme that acetylates acetyl-CoA synthetase in *Salmonella enterica*. *J Mol Biol* 340:1005–1012
- Starai VJ, Celic I, Cole RN, Boeke JD, Escalante-Semerena JC (2002) Sir2-dependent activation of acetyl-CoA synthetase by deacetylation of active lysine. *Science* 298:2390–2392
- Starai VJ, Takahashi H, Boeke JD, Escalante-Semerena JC (2003) Short-Chain fatty acid activation by acyl-coenzyme A synthetases requires SIR2 protein function in *Salmonella enterica* and *Saccharomyces cerevisiae*. *Genetics* 163:545–555
- Sterner DE, Berger SL (2000) Acetylation of histones and transcription-related factors. *Microbiol Mol Biol Rev* 64:435–459
- Thauer RK (1988) Citric-acid cycle, 50 years on. Modifications and an alternative pathway in anaerobic bacteria. *Eur J Biochem* 176:497–508
- Thauer RK, Möller-Zinkhan D, Spormann AM (1989) Biochemistry of acetate catabolism in anaerobic chemotrophic bacteria. *Annu Rev Microbiol* 43:43–67
- Thompson JD, Gibson TJ, Plewniak F, Jeanmougin F, Higgins DG (1997) The CLUSTAL_X windows interface: flexible strategies for multiple sequence alignment aided by quality analysis tools. *Nucleic Acids Res* 25:4876–4882
- Uhrigshardt H, Walden M, John H, Petersen A, Anemüller S (2002) Evidence for an operative glyoxylate cycle in the thermoacidophilic crenarchaeon *Sulfolobus acidocaldarius*. *FEBS Lett* 513:223–229
- Yamamoto J, Ikeda Y, Iguchi H, Fujino T, Tanaka T, Asaba H, Iwasaki S, Ioka RX, Kaneko IW, Magoori K, Takahashi S, Mori T, Sakaue H, Kodama T, Yanagisawa M, Yamamoto TT, Ito S, Sakai J (2004) A Krüppel-like factor KLF15 contributes fasting-induced transcriptional activation of mitochondrial acetyl-CoA synthetase gene AceCS2. *J Biol Chem* 279:16954–16962
- Zeiger CA, Randall DD (1991) Spinach leaf acetyl-coenzyme A synthetase: Purification and characterization. *Plant Physiol* 96:382–389
- Zhang P, Ng WV, DasSarma S (2003) Personal communication. <http://zdna2.umbi.umd.edu>, NSF grant reference (MCB-0135595)